LAWRENCE
LIVERMORE
NATIONAL
LABORATORY

LLNL-JRNL-604992

NDCX-II Target Experiments and Simulations

J. J. Barnard, R. M. More, M. Terry, A. Friedman, E. Henestroza, A. Koniges, J. W. Kwan, A. Ng, P. A. Ni, W. Liu, B. G. Logan, E. Startsev, A. Yuen

November 28, 2012

Nuclear Instruments and Methods in Physics Research A

Disclaimer

This document was prepared as an account of work sponsored by an agency of the United States government. Neither the United States government nor Lawrence Livermore National Security, LLC, nor any of their employees makes any warranty, expressed or implied, or assumes any legal liability or responsibility for the accuracy, completeness, or usefulness of any information, apparatus, product, or process disclosed, or represents that its use would not infringe privately owned rights. Reference herein to any specific commercial product, process, or service by trade name, trademark, manufacturer, or otherwise does not necessarily constitute or imply its endorsement, recommendation, or favoring by the United States government or Lawrence Livermore National Security, LLC. The views and opinions of authors expressed herein do not necessarily state or reflect those of the United States government or Lawrence Livermore National Security, LLC, and shall not be used for advertising or product endorsement purposes.

NDCX-II Target Experiments and Simulations

J. J. Barnard[1], R. M. More[1,2], M. Terry[1], A. Friedman[1], E. Henestroza[2], A. Koniges[2], J. W. Kwan[2], A. Ng[4], P. A. Ni[2], W. Liu[2], B.G. Logan[2], E. Startsev[3], A. Yuen[2]

1. Lawrence Livermore National Laboratory, Livermore CA, USA
2. Lawrence Berkeley National Laboratory, Berkeley, CA, USA
3. Princeton Plasma Physics Laboratory, Princeton, NJ, USA
4. University of British Columbia, BC, Canada

Abstract

The ion accelerator NDCX-II is undergoing commissioning at Lawrence Berkeley National Laboratory (LBNL). Its principal mission is to explore ion-driven High Energy Density Physics (HEDP) relevant to Inertial Fusion Energy (IFE) especially in the Warm Dense Matter (WDM) regime. We have carried out hydrodynamic simulations of beam-heated targets for parameters expected for the initial configuration of NDCX-II. For metal foils of order one micron thick (thin targets), the beam is predicted to heat the target in a timescale comparable to the hydrodynamic expansion time for experiments that infer material properties from measurements of the resulting rarefaction wave. We have also carried out hydrodynamic simulations of beam heating of metallic foam targets several tens of microns thick (thick targets) in which the ion range is shorter than the areal density of the material. In this case shock waves will form and we derive simple scaling laws for the efficiency of conversion of ion energy into kinetic energy of fluid flow. Geometries with a tamping layer may also be used to study the merging of a tamper shock with the end-of-range shock. This process can occur in tamped, direct drive IFE targets.

Introduction

The NDCX-II ion induction accelerator construction project [Waldron et al 2012] at LBNL was completed, and the machine is currently undergoing commissioning, which is planned for completion by June 2013 [Lidia et al 2012]. The purpose of NDCX-II is to explore ion-driven High Energy Density Physics (HEDP) relevant to Inertial Fusion Energy. NDCX-II is a low energy, high current, short pulse accelerator [Friedman et al 2010], that in many ways complements the high energy ion accelerators used for HEDP studies [Hoffmann et al 2000, Tahir et al 2005, 2007, Zhao et al 2009]. Using ions as drivers to create HEDP conditions has several attractive features, including spatially uniform and volumetric energy deposition over diagnosable large material volumes (~ one mm in radius by a few to tens of microns in depth) for any material or surface; precise control over energy deposition with an intrinsic energy spread of a few per cent; a small shot-to-shot variation in energy and intensity; the ability to do energy accounting by measuring the remaining beam after passage through thin foils; a benign environment for diagnostics (low debris and radiation background); high shot rates (~ two per minute); and energy deposition that can leave the target close to local thermodynamic equilibrium. At first NDCX-II will produce Li^+ ions at 1.2 MeV; a modest future extension is

envisioned that would raise the energy to 3 MeV. The beam is predicted to heat metal foils several microns thick in a timescale comparable to the hydrodynamic expansion time of the target for experiments that infer material properties from measurements of the rarefaction wave. Experiments using metallic foam targets several tens of microns thick wherein the beam creates shock waves will enable the inference of ion energy coupling into kinetic energy of fluid flow. Geometries with a tamping layer may be used to study the merging of a tamper shock with the end-of-range shock, a process that can occur in tamped direct drive IFE targets. We have carried out detailed hydrodynamic simulations of targets for several configurations, exploring how optical intensity measurements (from infrared to ultraviolet), laser doppler measurements (VISAR), and X-ray density measurements can be used to distinguish equations of state, and measure beam energy coupling in ion driven shock experiments.

NDCX-II will enable several types of measurements of heated matter and will be able to diagnose the target in several ways (see Bieniosek et al 2009, Ni et al 2009). Proposed experiments include: 1. Time dependent measurement of rarefaction waves and hydrodynamic expansion of the heated material. The measurements would include: a. temperature at the critical surface by photometry of the emission as a function of wavelength, emission angle, and polarization (polarization pyrometry) and time; b. velocity at the critical surface using Visar; and c. density as a function of position, by measurement of absorbed X-rays (created by an X-pinch or laser produced X-ray source). 2. Measurement of shock wave velocities, by imaging and timing of the breakout of the shockwave, and by measuring fluid velocities at the breakout time using VISAR, for those configurations in which shock waves are generated. 3. Electrical and thermal conductivity measurements, by measuring thermal breakout times of thin foils of various thicknesses, and B-field penetration times through heated matter. 4. Measurement of the final charge state and energy of the ions after passing through the target. One can measure both total energy in the beam pulse to determine the deposition and also the energy of the ions to ensure that the deposition mechanisms are understood. 5. Measurement of emission and absorption spectral lines of the heated target for investigation of atomic physics in the Warm Dense Matter regime. 6. Aerogel witness media to capture droplets and fragments from the exploding media. 7. Laser probe measurements to optically measure target light transmission, reflection and absorption by the ion heated target.

In addition to the general equation of state and shock physics experiments mentioned above there are other specific areas where NDCX-II will enable exploration. These areas include: 1. Liquid-vapor phase transition and the complete boundary between the regions and critical points. (The critical point is poorly known for many of the refractory metals). Solid-liquid phase transitions are also of interest for some material; 2. Phase transitions from metal to insulator and insulator to metal; 3.Transitions in opacity (for example, the transition between transparent and opaque, as in transient darkening that occurs in some materials in the Warm Dense Matter regime; 4. Fragmentation and fracture mechanics of materials under extreme conditions (e.g. carbon, silicon); 5. Droplet formation and the role of surface tension in rapidly expanding metals; 6. Ion beam stopping, scattering, and charge state evolution in heated material; 7. Unusual plasma configurations, such as

positive/negative ion plasmas (with very few free electrons) predicted to occur in halogens and some metals such as gold and platinum at temperatures near 0.4 eV.

Hydrodynamics driven by ion energy deposition for Heavy Ion Fusion

Heavy ion fusion is one of the principal options for inertial fusion energy (see e.g. Logan et al (2007), Hoffmann et al (2007), Horioka et al (2009), Sharkov et al (2007), and http://hif12.lbl.gov website). However, most inertial fusion target experiments to date have been carried out using laser beams. Lasers deposit their energy near the critical surface, roughly where the plasma frequency equals the laser frequency. In laser direct drive, as the ablator material and the critical surface expand outward and as the shockwave propagates inward, over the course of the pulse the shock front separates from the location of the energy deposition. In spherical heavy ion targets (see e.g. Meeker and Bangerter (1981), Tahir and Long (1986), Basko and Meyer-ter-Vehn (1993), Allshouse et al (1999), Someya et al (2006), Kawata et al (2007), Logan et al (2008), and Terry (2012)), and other heavy ion direct drive targets (such as fast ignition targets [Henestroza et al 2011, 2012]), ions deposit their energy volumetrically, and the ion mass and energy are chosen so that the ion range is a significant fraction of the ablator thickness. Moreover, accelerators offer a possibility of varying the ion energy over the course of the pulse. To maximize the shock strength it is possible to adjust the ion energy so that the ion range increases to keep up with the shock wave that was created during the initial stages of the pulse. Another option is to increase the intensity of the ion beam so that energy that arrives late in the pulse may overtake a shock launched at early times. How to maximize the shock intensity and optimize the conversion of ion energy into fuel fluid kinetic energy by varying the intensity and energy of the ion beam can be explored experimentally with the NDCX-II facility as well as theoretically as described below.

Shock strength maximization with ion beams involves determining optimum velocity tilt and focusing angle. The velocity tilt is the difference in velocity between the head and tail of the beam. . The velocity tilt is determined by adjusting the "triangular" induction voltage waveforms in the accelerator. The focusing angle is adjusted by varying the field strength of the final focusing solenoid and/or varying the radius at which the beam enters the solenoid. A large velocity tilt gives larger instantaneous range variation (larger variation in penetration depth), shorter pulse duration, larger chromatic variations (i.e. larger spot radii at the ends of the beam where the velocity difference relative to the midpulse is greatest.) A large focusing angle results in a smaller radius at the midpulse of beam, but larger chromatic variations (i.e. larger spot radii at the high velocity ends relative to the center of the beam.) For experiments involving rarefaction waves, the requirements of short pulse and maximum energy density lead to large velocity tilt at an optimum focusing angle. For experiments in which a shock is created, placing energy behind a shock implies the optimum may shift to longer pulses and smaller focusing angles. When a shock is created at the "end of range," there is a natural time scale for the shock to form, which is on the order of the distance from peak energy deposition to zero deposition divided by the sound speed. Shortening the duration below this time scale (but with the same fluence) does not enhance the shock strength or coupling efficiency.

Simulations of hydrodynamic experiments on NDCX-II.

When stopping in a single material in which the range is longer than the thickness of the material, ion beam deposition results in controlled, shock-free increases in temperature. However, when range of the ion beam is shorter than the target thickness, at the end of the ion range, at sufficient intensities, the strong pressure gradient will induce an "end-of-range" shock. For targets in which the ion beam crosses a material boundary, differential heating rates in the two materials will cause a pressure imbalance which can also drive a shock (the "tamper shock"). The tamper shock must be taken into account when designing IFE targets where the fuel is hydrodynamically coupled to the ion beam deposition region [Terry et al 2012]. The ion beams produced by NDCX-II will have sufficient range and intensity to experimentally study these phenomena. Simple layered targets should enable us to characterize the dynamics and spatial uniformity of these shocks. Various density profiles can be examined to study the tradeoff between tamping, and the increase of shock strength and the energy losses associated with heating the tamper.

In a homogeneous material, controlled volumetric energy deposition afforded by ion beams will allow us to investigate how to optimize the conversion of ion beam energy into kinetic energy of the target material. As discussed above, there are tradeoffs between pulse duration, velocity tilt and focusing angle. Because the ion energy deposition profile has a finite length (for example, for 10% Al foams the energy deposition has a scale length of order of 10 μ) the time to form a shock will be on the order of this distance divided by the sound speed (of order 10 ns for the 10% Al foam example). Figure 1 shows a simulation of a 1.2 MeV ion beam impinging upon 10% aluminum foam. The figure shows only the evolution of the fluid parameters along the central line. Since the thickness of the target is only 50 microns and the radial spot is of order 500 microns, to a good approximation the motion is one dimensional along the z direction at least for propagation distances of order 50 microns or less.

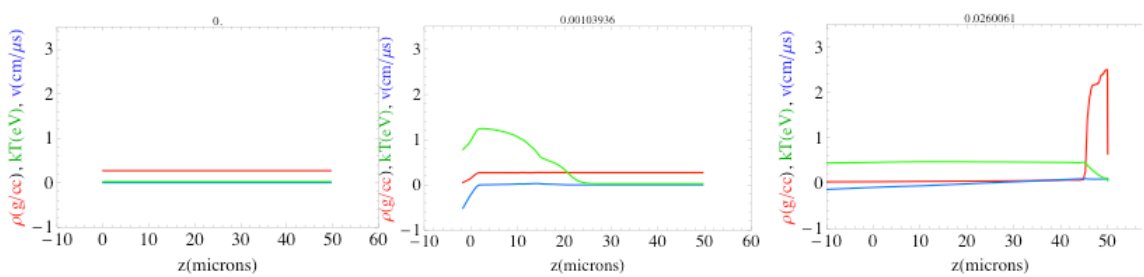

Figure 1. HYDRA simulation of the density ρ (red), temperature kT (green), and velocity v (blue), of the evolution of an ion beam heated target composed of Al at 10% solid density along the axis (r=0), at times t=0 (left), t=1 ns (center) and t= 26 ns, as a function of longitudinal position z. The 1.2 MeV ion beam (impinging upon the target from the left) had a pulse duration of 1 ns (initiated at t=0) and had a central fluence F (deposited energy per unit area, integrated over the pulse duration) of 12 J/cm^2.

As can be seen from Fig. 1, the ion deposition first raises the temperature, causing a leftward propagating rarefaction wave and a rightward propagating pressure wave that

steepens into a shock wave. Here the beam arrives from the left. The shock wave accelerates the unshocked mass ahead of the wave, and compresses it to liquid density (about 2.3 g/cm^3). The simulation was repeated for various total beam fluences (shown in fig. 2) and the trends plotted.

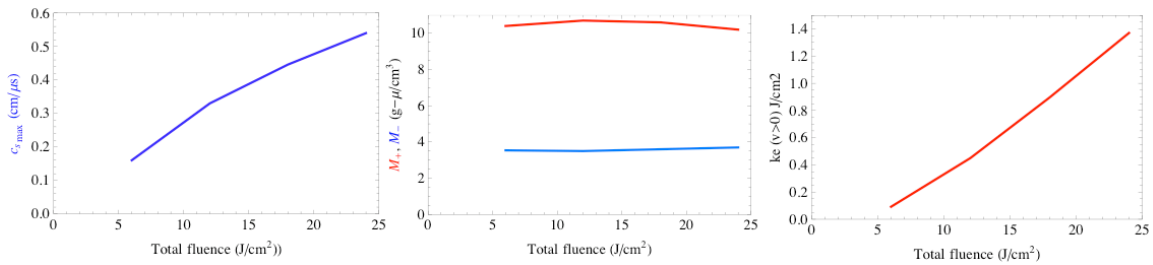

Figure 2. Left: Dependence on fluence F of maximum sound speed c_s; Center: accelerated mass (leftward moving mass M_- (red, upper line) and rightward moving mass M_+ (blue, lower line), and Right: fraction of integrated fluence converted into kinetic energy of the slab.

It is apparent from Fig. 2 that the mass per unit area that is ablated M_- (i.e. the mass that propagates in the simulation with negative velocity) is nearly independent of fluence. M_- is instead a fixed fraction f of the ion range. The ablation point where v=0 occurs at this fraction f of the ion range. In these simulations f is found to be of order 0.65. It is also apparent that the average velocity of the ablated material is very close to maximum sound speed created in the material from the beam heating. (The maximum speed occurs at the most negative point of the rarefaction wave and is typically a factor of 3 to 4 higher than the maximum sound speed. Figure 3 (left) shows the ratio α of the mass weighted average speed v_- (defined as the total momentum per unit area of the negative propagating fluid divided by M_-) to the maximum sound speed c_s. ($v_- = \alpha\, c_s$ where $\alpha \sim 1$).

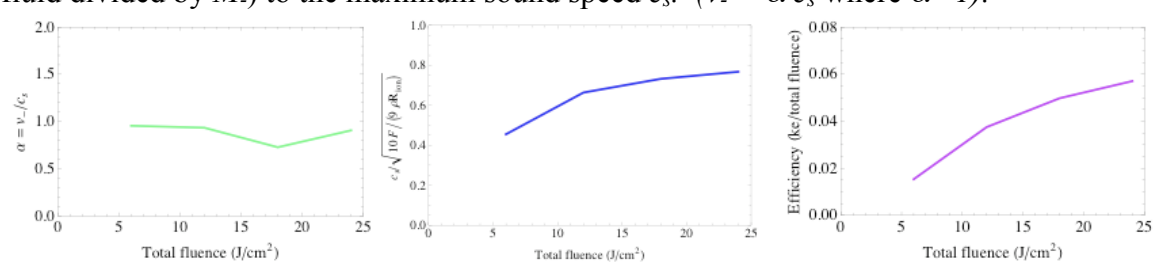

Figure 3. Left: α, ratio of average ablation speed v_- to maximum sound speed as a function of fluence for a 10% Al foam, using the LEOS equation of state. Center: c_s / $(10\, F/(9\, \rho R_{ion}))^{1/2}$ as a function of fluence. Right: Efficiency η of conversion of beam energy into fluid flow energy, $M_+ v_+^2/(2F)$.

Another important quantity is the ratio of the sound speed to the deposited energy density per unit mass. In general, the square of the sound speed c_s^2 is defined as the partial derivative of the pressure P with respect to density ρ at constant entropy S, $c_s^2 = \partial P/\partial\rho\,|_S$, which can be written in terms of the ratio of specific heats γ as $c_s^2 = \gamma P/\rho$. Similarly, the energy density per unit mass ε may be written $\varepsilon = P/(\rho(\gamma-1))$ so that alternatively the

square of the sound speed may be given by $c_s^2 = \gamma(\gamma-1)\varepsilon \cong \gamma(\gamma-1)\Delta\varepsilon$. Here, $\Delta\varepsilon$ is the change in internal energy density resulting from the ion beam heating. The approximate inequality above assumes that the temperature after beam heating is much greater than the initial temperature. Here the factor $\gamma(\gamma-1)$ includes all of the physical details arising from a particular equation of state, including the latent heat of fusion (melting) and the heat of vaporization of the foam or solid. For a monatomic perfect gas γ=5/3, so in that case $\gamma(\gamma\text{-}1) = 10/9 \cong 1.1$. We expect at lower intensities (smaller F), the melting and vaporization energies will be significant so the effective γ will be closer to 1, and thus $\gamma(\gamma\text{-}1)$ will be < 1. As F increases, $\gamma(\gamma\text{-}1)$ approaches 10/9 (as long as F is low enough that ionization is not important). We may approximate $\Delta\varepsilon \approx F / \rho R_{ion}$. Here ρR_{ion} is the range of the ion beam (in units of mass/unit area) and is approximately 5.4 g/cm^2 for the 1.2 MeV Li^+ ion beam stopping in Al, based on the stopping model used in HYDRA. In figure 3 (center), we plot the ratio of $c_s /(10\ F /(\ 9\ \rho R_{ion}))^{1/2}$ found from the simulations and, as expected, this ratio tends toward unity as F increases.

We may estimate the efficiency η of the conversion of beam energy into kinetic energy of the accelerated mass by noting that total mass and momentum is conserved. Mass conservation implies:

$$\rho R_{tot} = \sum_{i:v<0} \rho_i \Delta z_i + \sum_{i:v>0} \rho_i \Delta z_i \equiv M_- + M_+ = f\rho R_{ion} + M_+ \quad \Rightarrow \quad M_+ = \rho R_{tot} - f\rho R_{ion} \tag{1}$$

where ρR_{tot} is the total mass per unit area of the target. Momentum conservation implies:

$$0 = \sum_{i:v<0} \rho_i v_i \Delta z_i + \sum_{i:v>0} \rho_i v_i \Delta z_i \equiv M_- v_- + M_+ v_+ = -\alpha \left(\frac{\gamma(\gamma-1)F}{\rho R_{ion}} \right)^{1/2} f\rho R_{ion} + (\rho R_{tot} - f\rho R_{ion}) v_+ \tag{2}$$

$$\Rightarrow v_+ = \frac{\alpha f \left(\gamma(\gamma-1)\rho R_{ion} F\right)^{1/2}}{(\rho R_{tot} - f\rho R_{ion})}$$

The coupling efficiency η is defined as $\eta = M_+ v_+^2/(2\ F)$. Using eq. (2) this implies,

$$\eta = \frac{\alpha^2 f^2 \gamma(\gamma-1)}{2(\rho R_{tot} / \rho R_{ion} - f)} \tag{3}$$

In eq. (3) the fluence F does not explicitly appear, but η will depend on F through γ. Eq. (3) will become inaccurate as $\rho R_{\text{tot}}/\ \rho R_{\text{ion}}$ approaches 1 (if $\rho R_{\text{tot}}/\ \rho R_{\text{ion}} < 1$, part of the beam energy passes through the target). This formula suggests that for fluences of order 10 J/cm^2 coupling efficiencies around 6% are expected (for $\rho R_{\text{tot}}/\ \rho R_{\text{ion}} = 2.5$, $\alpha = 1$, $f = 0.65$, and $c_s\ /\ (10\ F\ /(9\ \rho R_{ion}))^{1/2} = 0.7$ (i.e. $\gamma(\gamma-1) \cong 0.7^2(10/9) \cong 0.54$). For $\rho R_{\text{tot}}/\ \rho R_{\text{ion}} > 2.5$ the scaling indicates the efficiency will decrease with increasing ρR_{tot} and with decreasing ρR_{tot} there will be some increase in the efficiency until the ρR_{tot} either does not stop the entire ion beam or the swept mass does not persist at liquid density. The estimate pertains to the time when the shock reaches the end of the foil. In subsequent time, further evolution of the accelerated mass can occur (arising from processes such as evaporation, or further acceleration from the asymmetric temperature profile, or break up into droplets). With NDCX-II we may validate this estimate and in addition determine how pulse duration, foam density, velocity tilt and other factors will affect the coupling efficiency.

Tamped targets

Tamping to confine energy and raise pressure is a common technique in the design of munitions driven by chemical explosives. Tampers have also been proposed for spherical heavy ion fusion targets (Terry et al 2012). Tampers are regions of dense material that surround the ablator and increase the pressure in the ablator by inhibiting the expansion of the ablator material and thus enhancing the ion energy coupling into fuel kinetic energy. (In some cases, the dense material can act as a hohlraum, reflecting and homogenizing the radiation that impinges upon the ablator, allowing hybrids that combine aspects of both direct and indirect drive.) The ion beam must have a long enough range to pass through the tamper. Energy deposition in the tamper reduces the energy arriving at the ablator. At the interface between tamper and the lower density ablator, a pressure discontinuity creates a shock wave that propagates into the ablator. The shock wave that forms at the end of the ion range (in the ablator) propagates at a lower velocity than the tamper shock, and so the tamper shock can catch the end-of-range shock. The thickness and densities of the tamper and ablator should be designed to optimize the coupling efficiency. We have begun to explore these effects computationally as shown in fig. 4, in anticipation of doing future experiments on NDCX-II.

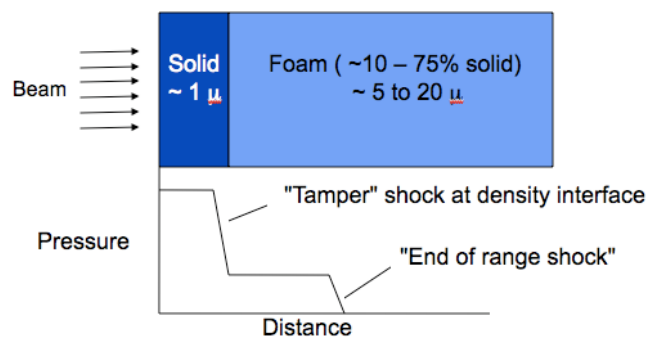

Figure 4. Schematic of tamped target experimental setup.

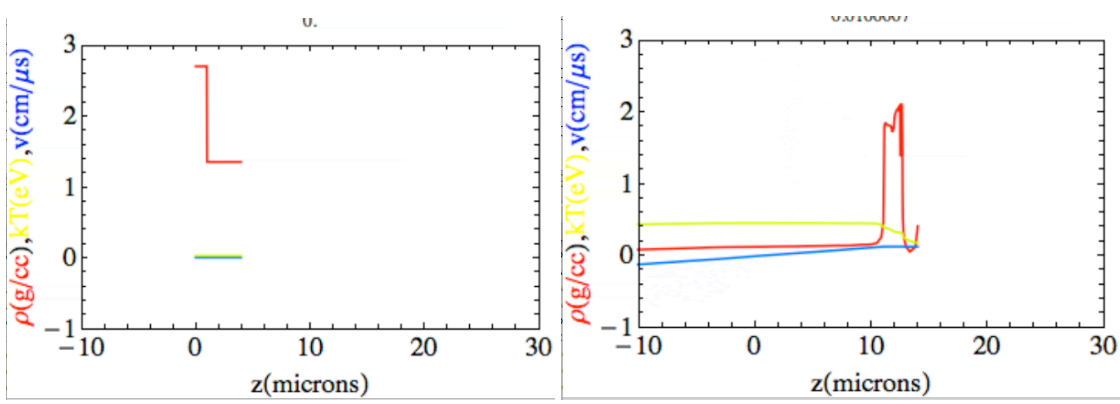

Figure 5. HYDRA simulation of a beam heated tamped aluminum target with 1 micron solid tamper followed by 4 microns of 50% metallic foam Al. The initial density (red) at beam center as a function of longitudinal position z is shown at left, and the resulting acceleration of a slab at near liquid density is shown at right after 10 ns. The temperature

profile is shown in yellow and velocity profile in blue. (The initial velocity and temperature overlay in the figure, appearing green). The final velocity was about 0.1 cm/μs in the example.

Rarefaction waves

When the range of the ion beam exceeds the thickness of the material being heated (thin targets), the material can be heated quite uniformly. If the timescale is sufficiently short, and the ion energy is slightly above the peak energy in dE/dX (the Bragg peak) when it enters the foil and slightly below the Bragg peak when it exits the foil the resulting temperature will be quite uniform, as the local temperature will be proportional to dE/dX. Over time a rarefaction wave propagates towards the longitudinal center of the foil, and the heated material propagates rapidly outward at speeds characteristic of the sound speed. For beam parameters expected for NDCX-II, it will be possible to measure the characteristics of these rarefaction waves in ion heated metallic foils and foams (for EOS and hydrodynamic studies relevant to initial stages of IFE targets) via pyrometry, imaging, VISAR, and/or X-ray imaging diagnostics [*cf* Barnard et al 2007, 2009, 2010, Yuen et al, 2012]. By comparing the temperature, velocity, and density information obtained from these diagnostics against those of hydrodynamic simulations with different candidate equations of state we may confirm the validity of candidate equations of state. Although the initial energy of NDCX-II will be below the Bragg peak for most materials and the hydrodynamic timescale will be somewhat shorter than the pulse duration, simulations show that approximately uniform conditions will still be created (see fig. 6). Fig. 7 shows an ALE-AMR simulation of the expanding foil for NDCX-II parameters. ALE-AMR is a multi-dimensional hydrodynamics code that includes some physics not available in HYDRA such as mesh refinement. Models for surface tension effects are currently being developed for inclusion into ALE-AMR [Liu et al 2012].

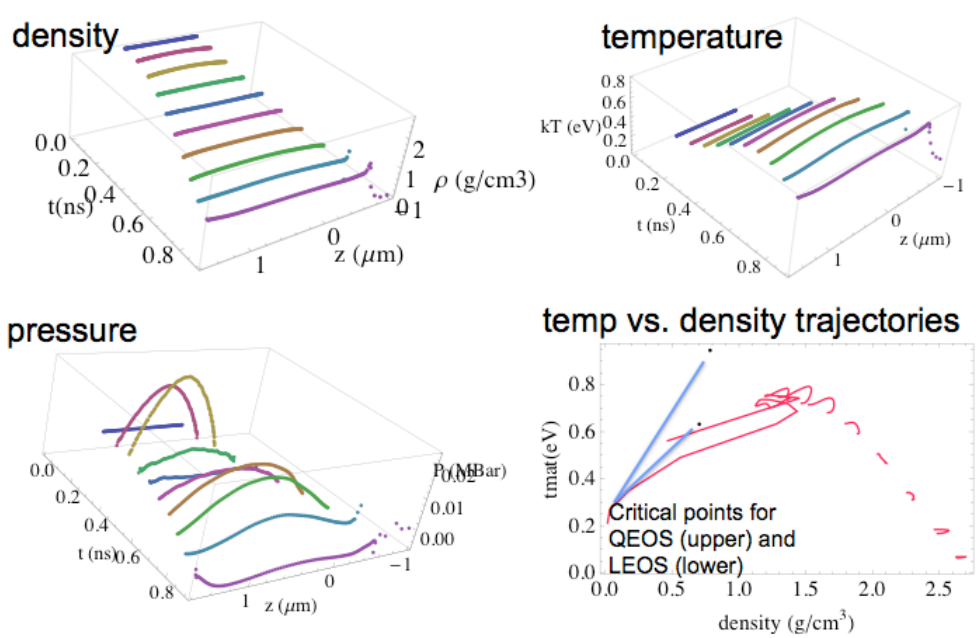

Figure 6. HYDRA simulation of a 1.2 MeV Li+ ion beam impinging on a 1 micron aluminum foil. The fluence was 8.4 J/cm^2 delivered in 0.85 ns. Upper left: Density r at

the center of the foil as a function of longitudinal position z, for ten different snapshots in time t. Upper right: Temperature kT vs z and t. Lower left: pressure vs z and t. Lower right: temperature vs density for each of the snapshots. (The two points are the critical points for QEOS (More et al 1985) and LEOS, two commonly used Equations of State.)

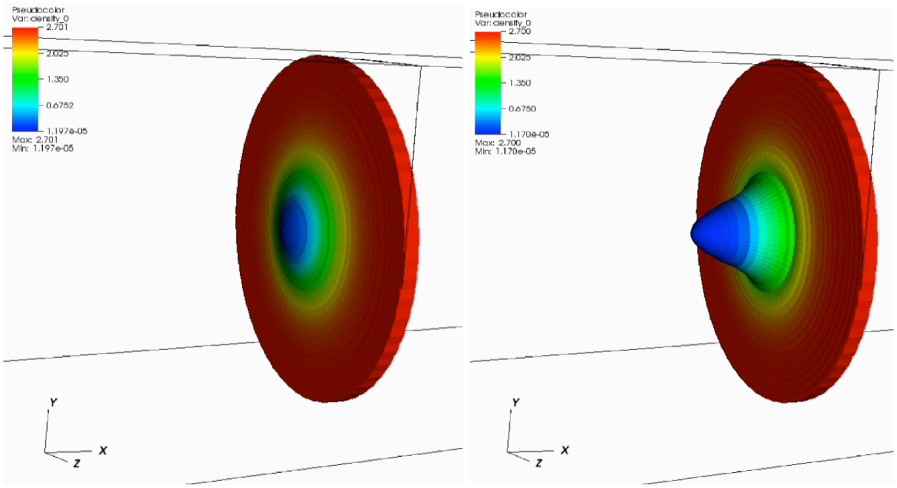

Figure 7. ALE-AMR 2D simulation of thin foil heating experiment after the completion of the heating pulse (left) at 0.85 ns and (right) after at 1.70 ns. Density contours are shown in color. The longitudinal scale is exaggerated relative to the transverse. The radius of the simulated target is 1 mm, while the thickness of the original target is 1.0 mm.

Conclusion and discussion

NDCX-II is a new ion induction accelerator undergoing commissioning at Lawrence Berkeley National Laboratory. It will have capabilities that will allow experiments in the Warm Dense Matter regime that are relevant to inertial fusion energy and basic science of ion stopping, conductivity, and hydrodynamics in heated material. We have simulated thin target experiments in which heated matter of relatively high initial uniformity evolves via rarefaction waves that can be used to infer material properties such as the liquid-vapor critical point and discriminate between equations of state. We have also simulated "thick" target experiments that exemplify how shocks generated on NDCX-II will enable experiments that optimize ion coupling, an area of interest for heavy ion fusion. For simple homogeneous targets, we have estimated the coupling efficiency (conversion of ion beam energy into kinetic energy of the accelerated liquid density material) and plan to extend the study to evaluate the effect on efficiency of pulse duration, energy tilt and mass distribution, including the case of tamped targets.

References

G. O. Allshouse, R. E. Olson, D. A. Callahan-Miller, M. Tabak, "Deposition and drive symmetry for light ion fusion," Nuc. Fus. 39, 893 (1999).

J. J. Barnard, J. Armijo, R. M. More, A. Friedman, I. Kaganovich, B. G. Logan, M. M.

Marinak, G. E. Penn, A. B. Sefkow, P. Santhanam, P. Stoltz, S. Veitzer, J .S. Wurtele, "Theory and Simulation of Warm Dense Matter Targets," Nuclear Instruments and Methods in Physics Research A 577, (2007), 275-283.

J. J. Barnard, J. Armijo, D. S. Bailey, A. Friedman, F. M. Bieniosek, E. Henestroza, I. Kaganovich, P. T. Leung, B. G. Logan, M.M. Marinak, R. M. More, S. F. Ng, G. E. Penn, L. J. Perkins, S. Veitzer, J. S. Wurtele, S. S. Yu, A. B. Zylstra, "Ion beam heated target simulations for warm dense matter physics and inertial fusion energy," Nuclear Instruments and Methods in Physics Research A 606, 134-138, (2009).

J. J. Barnard, J. Armijo, F. M. Bieniosek, A. Friedman, M. Hay, E. Henestroza, B. G. Logan, R. M. More, P. A. Ni, L. J. Perkins, S-F. Ng, J.S. Wurtele, S.S. Yu, A. B. Zylstra, "Simulations for experimental study of warm dense matter and inertial fusion energy applications on NDCX-II," IFSA 2009, Journal of Physics Conference Series, Vol 244, Part 3, 032027 (2010). doi: 10.1088/1742-6596/244/3/032027

M. M. Basko and J. Meyer-ter-Vehn, "Hohlraum target for heavy ion inertial fusion," Nuclear Fusion, Vol. 33, No. 4 (1993) 601.

F. M. Bieniosek, J.J. Barnard, M.A. Leitner, A.W. Molvik, R. M. More, P. K. Roy, "Diagnostics for near-term warm dense matter experiments," Nuclear Instruments and Methods in Physics Research A, **577**, 284 (2007)

F. M. Bieniosek, E. Henestroza, M.A. Leitner, B.G. Logan, R. M. More, P. K. Roy, P. Ni, P.A. Seidl, W.L. Waldron, J. J. Barnard, "High energy density physics experiments with intense heavy ion beams," Nuclear Instruments and Methods in Physics Research A, **606**, 146 (2009)

A. Friedman, J.J. Barnard, R.H. Cohen, D.P. Grote, S.M. Lund, W.M. Sharp, A. Faltens, E. Henestroza, J.-Y. Jung, J.W. Kwan, E.P. Lee, M.A. Leitner, B.G. Logan, J.-L. Vay, W.L. Waldron, R.C. Davidson, M. Dorf, E.P. Gilson, and I.D. Kaganovich," Beam dynamics of the Neutralized Drift Compression Experiment-II, a novel pulse-compressing ion accelerator," Phys. Plasmas 17, 056704 (2010).

E. Henestroza, B.G. Logan, L. J. Perkins, "Quasispherical fuel compression and fast ignition in a heavy-ion-driven X-target with one-sided illumination," Physics of Plasmas **18**, 032702, (2011)

E. Henestroza and B. G. Logan, "Progress towards a high-gain and robust target design for heavy ion fusion", Physics of Plasmas **19**, 072706 (2012).

D.H.H. Hoffmann, R. Bock, A.Ya. Faenov, U. Funk, M. Geissel, U. Neuner, T.A. Pikuz, F. Rosmej, M. Roth, W. Süß, N. Tahir, A. Tauschwitz, "Plasma physics with intense laser and ion beams," Nucl. Instrum. Methods Phys. Res. B 161-163, 9 (2000).

D.H.H. Hoffmann, A. Blazevic, S. Korostiy, P. Ni, S.A. Pikuz, B. Rethfeld, O. Rosmej,

M. Roth, N.A. Tahir, S. Udrea, D. Varentsov, K. Weyrich, B.Yu. Sharkov, Y. Maron, "Inertial fusion energy issues of intense heavy ion and laser beams interacting with ionized matter studied at GSI-Darmstadt," Nuclear Instruments and Methods in Physics Research A 577, 8 (2007).

K. Horioka, T. Kawamura, M. Nakajima, K. Kondo, M. Ogawa, Y. Oguri, J. Hasegawa, S. Kawata, T. Kikuchi, T. Sasaki, M. Murakami, K. Takayama, "Activities on heavy ion inertial fusion and beam-driven high energy density science in Japan," Nuclear Instruments and Methods in Physics Research A, 606, 1 (2009).

S. Kawata, K. Miyazawa, T. Kikuchi, T. Someya, "Direct–indirect mixed implosion mode in heavy ion inertial fusion," Nucl. Inst. in Phys. Res. A, 577, 332-336 (2007)

A. E. Koniges, N. D. Masters, A. C. Fisher, R. W. Anderson, D. C. Eder, T. B. Kaiser, D. S. Bailey, B. Gunney, P. Wang, B. Brown, K. Fisher, F. Hansen, B. R. Maddox, D. J. Benson, M. Meyers and A. Geille, "ALE-AMR: A new 3D multi-physics code for modeling laser/target effects," Journal of Physics: Conference Series, 244, 032019 (2010).

S. Lidia, D. Arbelaez, W. Greenway, J.-Y. Jung, J. Kwan, T. Lipton, A. Pekedis, P. Roy, P. Seidl, J. Takakuwa, W. Waldron, A. Friedman, D. Grote, W. Sharp, E. Gilson, "Initial commissioning of NDCX-II," *Proceedings of IPAC2012, New Orleans, Louisiana, USA*, MOEPPB005, (2012).

W. Liu, J. Barnard, A. Koniges, D. Eder, A. Friedman, A. Fisher, and N. Masters, "Using a Korteweg-type model for modeling surface tension and its applications," Bulletin of the American Physical Society, Vol. 57, No. 12, Abstract BP8.00058 (2012). Also, W. Liu et al, manuscript in preparation (2012).

B.G. Logan, F.M. Bieniosek, C.M. Celata, J. Coleman, W. Greenway, E. Henestroza, J.W. Kwan, E.P. Lee, M. Leitner, P.K. Roy, P.A. Seidl, J.-L. Vay, W.L. Waldron, S.S. Yu, J.J. Barnard, R.H. Cohen, A. Friedman, D.P. Grote, M. Kireeff Covo, A.W. Molvik, S.M. Lund, W.R. Meier, W. Sharp, R.C. Davidson, P.C. Efthimion, E.P. Gilson, L. Grishamc, I.D. Kaganovichc, H. Qinc, A.B. Sefkowc, E.A. Startsev, D. Welch, C. Olson, "Recent U.S. advances in ion-beam-driven high energy density physics and heavy ion fusion," Nuclear Instruments and Methods in Physics Research A 577, 1 (2007).

B. G. Logan, L. J. Perkins, and J. J. Barnard. "Direct Drive Heavy-Ion-Beam Inertial Fusion at High Coupling Efficiency," Phys. Plasmas, 15:072701, (2008).

M.M. Marinak, G.D. Kerbel, N.A. Gentile, O. Jones, D. Munro, S. Pollaine, T.R. Dittrich, S.W. Haan, "Three-Dimensional Simulations of National Ignition Facility Targets," Physics of Plasmas, 8, 2275 (2001).

D. J. Meeker and R. O. Bangerter, "A Tamped Split-Fuel-Layer Ion-Beam Target," Laser Program Annual Report 1981, Lawrence Livermore National Laboratory, UCRL-50021-

81, 3-15 (1982).

R. More, K. Warren, D. Young and G.B. Zimmerman, "A New Quotidian Equation of State (QEOS) for Hot Dense Matter," Phys. Fluids 31, 3059 (1988).

P. A. Ni, F. M. Bieniosek, M. Leitner, C. Weber, W.L. Waldron, "Testing of optical diagnostics for ion-beam-driven WDM experiments at NDCX-I," Nuclear Instruments and Methods in Physics Research A, **606**, 169 (2009).

B. Yu. Sharkov, "Overview of Russian heavy-ion inertial fusion energy program," Nuclear Instruments and Methods in Physics Research A 577, 8 (2007).

T. Someya, K. Miyazawa, T. Kikuchi, S. Kawata, "Direct-indirect mixture implosion in heavy ion fusion,"Laser Part. Beam 24, 359-369 (2006).

N. A. Tahir and K. A. Long, "Importance of radiation effects in ion-beam-driven inertial fusion target calculations: Compensation of range shortening by radiation transport in ion-beam-generated plasmas," Phys. Fluids, Vol. 29, No. 4 (1986) 1282.

N.A. Tahir, C. Deutsch, V. E. Fortov, V. Gryaznov, D. H. H. Hoffmann, M. Kulish, I. V. Lomonosov, V. Mintsev, P. Ni, D. Nikolaev, A. R. Piriz, N. Shilkin, P. Spiller, A. Shutov, M. Temporal, V. Ternovoi, S. Udrea, and D. Varentsov, "Proposal for the Study of Thermophysical Properties of High-Energy-Density Matter Using Current and Future Heavy-Ion Accelerator Facilities at GSI Darmstadt," Physical Review Letters, **95** 035001 (2005).

N.A. Tahir, P. Spiller, A. Shutov, I. V. Lomonosov, V. Gryaznov, A. R. Piriz, G. Wouchuk, C. Deutsch, V. E. Fortov, D. H. H. Hoffmann, R. Schmidt, " HEDgeHOB: High-energy density matter generated by heavy ion beams at the future facility for antiprotons and ion research," Nucl. Instr. and Meth. A 577 (2007) 238.

M. Terry et al, "High Efficiency Heavy Ion ICF Targets using Tamped Pusher and X-ray Ablation Drive," in preparation, 2012.

W.L. Waldron, W.J. Abraham, D. Arbelaez, W.G. Greenway, J.-Y. Jung, J.W. Kwan, M.L. Leitner, S.M. Lidia, T.M. Lipton, L.R. Reginato, M.J. Regis, P.K. Roy, M.W. Stettler, J.H. Takakuwa, J. Volmering, V.K. Vytla, "The NDCX-II Engineering Design," Nuclear Instruments and Methods in Physics Research," this issue (2013).

A. Yuen, J. J. Barnard, R. M. More, "Rarefaction Waves in Van der Waals Fluids," Bulletin of the American Physical Society Division of Plasma Physics, Vol 56, No. 16, Abstract PP9.00078 (2011). Also Yuen et al, manuscript in preparation (2012).

Y. Zhao, G. Xiao, H. Xu, H. Zhao, J. Xia, G. Jin, X. Ma, Y. Liu, P. Zhang, Y. Wang, D. Li, H. Zhao, W. Zhan, Z. Xu, D. Zhao, F. Li, X. Chen, "An outlook of heavy ion driven

plasma research at IMP-Lanzhou," Nuclear Instruments and Methods in Physics Research B: Beam Interactions with Materials and Atoms, **267**, 163 (2009).

Prepared by LLNL under Contract DE-AC52-07NA27344.